Original Article

A multiomic ferroptosis-associated prognostic signature incorporating epigenetic and transcriptional biomarkers for hepatocellular carcinoma

Jida Chen[1], Xinli Zhu[2], Danzhi Chen[1], Lidan Jin[1], Wenbo Xu[1], Wei Yu[1], Liwen Zhang[1]

[1]Department of Surgical Oncology, Affiliated Sir Run Run Shaw Hospital, Zhejiang University School of Medicine, Hangzhou, China; [2]Department of Radiotherapy, First Affiliated Hospital, Zhejiang University School of Medicine, Hangzhou, China

Contributions: (I) Conception and design: J Chen; (II) Administrative support: J Chen; (III) Provision of study materials or patients: J Chen, X Zhu; (IV) Collection and assembly of data: D Chen, L Jin; (V) Data analysis and interpretation: J Chen, W Xu; (VI) Manuscript writing: All authors; (VII) Final approval of manuscript: All authors.

Correspondence to: Jida Chen, MD. Department of Surgical Oncology, Affiliated Sir Run Run Shaw Hospital, Zhejiang University School of Medicine, Hangzhou 310000, China. Email: 3305052@zju.edu.cn.

Background: Ferroptosis was reported to have tremendous promise in the treatment and prognosis of hepatocellular carcinoma (HCC). Here, we identified a novel ferroptosis-related prognostic signature incorporating epigenetic and transcriptional biomarkers could help predicting survival of patients with HCC.

Methods: We employed multi-omics and clinical data from The Cancer Genome Atlas (TCGA) database to identify the ferroptosis-associated methylation CpG sites associated with HCC survival using sure independence screening (SIS). Then we utilized Kaplan-Meier curves to evaluate the prognostic significance of gene expression and DNA methylation. Receiver operating characteristic (ROC) curve was used predicting the 3- and 5-year survival. Mediation analysis of ferroptosis-related methylation and transcriptional score was performed.

Results: We firstly identified 114 significant CpG sites under the criteria of false discovery rate (FDR) <0.05 in training set. Then we screened out 5 candidate CpG sites in validation set for multivariate screening and stepwise regression. We found that the high-risk group had significantly shorter survival time than the low-risk group in the prognostic signature combined with epigenetic and transcriptional scores (HR =2.72 95% CI: 2.01–3.68, P=8.75E-11). And the predictive model involving clinical information, gene expression, and methylation data performed best for 3-year survival prediction (AUC =0.672) and 5-year survival prediction (AUC =0.742).

Conclusions: Our results suggested a signature combining clinical information, ferroptosis-related gene expression, and methylation presented a superior ability for prognostic prediction in HCC, which may bring us novel tool and targets in the treatment of HCC.

Keywords: Hepatocellular carcinoma (HCC); ferroptosis; methylation; transcription; overall survival

Submitted Dec 25, 2021. Accepted for publication Apr 27, 2022.
doi: 10.21037/tcr-21-2882
View this article at: https://dx.doi.org/10.21037/tcr-21-2882

Introduction

Primary liver cancer is the third leading cause of cancer-related death worldwide, affecting 905,677 individuals and causing 830,180 deaths according to global cancer statistics in 2020 (1). Hepatocellular carcinoma (HCC) comprises approximately 75% to 85% of all liver cancer cases. The overall 5-year survival rate of HCC varies from 5.1% to 20% (2-4). Classic serum biomarkers like alpha-fetal protein (AFP) and epithelial cell adhesion molecule (EpCAM) could help in the diagnosis and monitoring of the HCC (5), but

the sensitivity and specificity are limited. The considerable diversity of prognosis underlines the complexity of HCC, which might stem from the variation of genetic alterations and epigenetic modifications (6). However, few studies were reported in the genetic and epigenetic biomarkers in the prediction of outcomes in HCC.

Ferroptosis, a newly identified form of non-apoptosis-regulated cell death with distinct morphological and mechanistic changes (7), causes cell death by producing reactive oxygen species (ROS) from iron overload and lipid hydroperoxides accumulation (8,9). Previous studies suggested that targeting ferroptosis-related genes could sensitizing cancer cells to ferroptosis and subsequently suppressing tumor growth in HCC (10-12). For instance, TP53 could sensitize hepatic cancer cells to ferroptosis via SLC7A11 (13), P62 could sensitize hepatic cancer cells to ferroptosis induced by sorafenib via NRF2 (14). Therefore, ferroptosis plays an important role during cancer progression and treatment, suggesting the tremendous promise of ferroptosis regulator genes (FRGs) signatures in the prognosis prediction and treatment of HCC.

DNA methylation could regulate the expression of FRGs in tumors (15). Aberrant methylation CpG sites have been considered as potential prognostic factors for cancer patients (16). These findings provide new avenues to detect prognostic biomarkers across different omics in HCC, however, most studies of ferroptosis-related biomarkers for HCC prognosis focus on single-omic data, the interactions between multi-omics data were not mentioned (17,18). Therefore, it will be interesting to consider the prognostic value of ferroptosis-related biomarkers at both epigenetic and transcriptomic levels in HCC.

In the present study, we employed multi-omics and clinical data from The Cancer Genome Atlas (TCGA) database to investigate the prognostic effect of ferroptosis-related methylation biomarkers and corresponding gene expression for overall survival in HCC patients. We further generated a ferroptosis-related prognostic model incorporating epigenetic, transcriptomic data and clinical variables for survival prediction of HCC patients. We present the following article in accordance with the TRIPOD reporting checklist (available at https://tcr.amegroups.com/article/view/10.21037/tcr-21-2882/rc).

Methods

Study population and datasets

Ferroptosis-related DNA methylation data and clinical information of HCC patients were downloaded from the TCGA database (19) (https://cancergenome.nih.gov/). Besides, we also downloaded gene expression data to identify the potential underlying biological mechanisms. The RNA-seq data were generated from Affymetrix Human Genome U133A 2.0 (GPL3921). A total of 375 HCC patients were included in the present study. Only patients with survival information were included in this study. We obtained 60 ferroptosis-related genes from the previous literature (17) (Table S1). A total of 1,035 ferroptosis-related DNA methylation sites were annotated. An additional validation set (GSE14520) was downloaded from the GEO database (20) (https://www.ncbi.nlm.nih.gov/geo/query/acc.cgi?acc=GSE14520), which only included clinical information and RNA-seq data of 221 HCC patients. The RNA-seq data were generated from Affymetrix GeneChip HG-U133A 2.0 arrays (GPL571 and GPL3921 platforms). The clinical information including study dates, eligibility criteria, et al were in line with the published literatures (19,20). The sample size was estimated using nQuery Advisor 6.01 (Statistical Solutions Ltd., MA, USA) software. A sample size of 300 participants could reach 95% power of study (two-sided α=0.05).

The development of ferroptosis-related DNA methylation signature

We randomly assigned samples into a training set and a validation set with a ratio of 2:1. In the training set, univariate Cox model was used to select candidate CpG sites related to survival and false discovery rate (FDR) <0.05 was considered as statistically significant. Consider the overfitting problem of high-dimensional microarray data due to the small sample size (21), we performed sure independence screening (SIS) (22) variable selection, which is based on Least Absolute Shrinkage and Selection Operator (LASSO) Cox penalized regression to identify candidate CpG sites and to construct a multi-CpG-based classifier predicting overall survival, through the R package "SIS". Then, the candidate CpG sites selected by SIS method were then included in a multivariate Cox proportional hazards model, and statistically significant CpG sites were selected by stepwise regression. Finally, the selected CpG sites were used to develop the signature. The whole design was depicted in *Figure 1*.

Statistical analysis

Overall survival was set as primary endpoint, 3- and 5-year

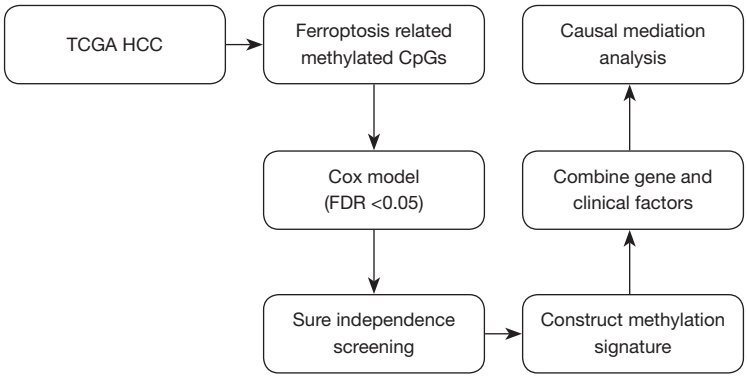

Figure 1 A schematic depiction of study design and statistical analysis. TCGA, The Cancer Genome Atlas; HCC, hepatocellular carcinoma; FDR, false discovery rate.

survival were used as secondary endpoint in this study. Continuous variables were described as mean ± standard deviation (SD) and categorized variables were expressed in frequency (n) and proportion (%).

We utilized Kaplan-Meier curves to display the prognostic significance of gene expression or DNA methylation, log-rank test was used to evaluate the difference. We also predicted the 3- and 5-year survival for patients using Nearest Neighbor Estimation (NNE) method (23). A receiver operating characteristic (ROC) curve was computed to present the prediction accuracy using the R package "survivalROC".

To identify whether DNA methylation could affect the expression of corresponding genes, we estimated the Pearson's correlation between gene expression and methylation.

We performed mediation analysis to explore potential "ferroptosis-related DNA methylation → gene expression → HCC survival" pathway (24), which meant whether the ferroptosis-related prognostic effect of DNA methylation sites is mediated by affecting corresponding mRNA expression. Adjusting for age, gender and clinical stage, the total effect of methylation on survival (HRtotal) was divided into indirect effects (HRindirect) and direct effects (HRdirect). HRindirect represented the indirect effect of methylation on survival mediated through gene expression and HRdirect represented the direct effect of methylation on survival (25). All P values in this study were two-sided, and P<0.05 was considered statistically significant. All statistical analyses were performed applying the R version 4.0.3 (R Foundation), unless otherwise specified.

Ethical statement

The study was conducted in accordance with the Declaration of Helsinki (as revised in 2013).

Results

Ferroptosis-related signature for HCC prognosis

Clinical variates for the HCC patients, including the overall survival, race, gender, age, and tumor stage, was described in *Table 1*. The average age of all subjects was 59.55 years, and among these patients, 32.3% were female, about half of them (49.9%) were white. Two hundred and fifty patients were included in the training set and 125 patients were enrolled in the validation set. An additional validation set (GSE14520) was downloaded from the GEO database (20), which included 221 HCC patients. The baseline information was listed in *Table 1*.

In the training set, we first identified 114 significant CpG sites significantly associated with overall survival of HCC under the criteria of FDR <0.05. The identified CpG sites were further validated in the validation set. Further, five validated CpG sites were analyzed using SIS method and stepwise regression (cg02916418, cg05373863, cg13028471, cg07137701, cg15044146, details in Table S2) to construct the ferroptosis-related methylation score. The ferroptosis-related methylation score was established employing5 CpGs and their regression coefficients, which was calculated as following: $Score_{methylation}$ =−2.69× cg02916418−6.69× cg05373863−12.15× cg13028471−29.88× cg07137701+5.97× cg15044146. The corresponding genes of these CpGs

Table 1 Demographic characteristics of the HCC patients in this study

Characteristic	Total, LIHC (N=375)	Training set, LIHC (N=250)	Validation set, LIHC (N=125)	GSE14520 (N=221)
Age, years, mean ± SD	59.55±13.40	59.20±13.80	60.26±12.60	50.81±10.62
Gender, n (%)				
Female	121 (32.3)	78 (31.2)	43 (34.4)	30 (13.6)
Male	254 (67.7)	172 (68.8)	82 (65.6)	191 (86.4)
Pathologic stage*, n (%)				
I	175 (46.7)	120 (48.0)	55 (44.0)	93 (42.1)
II	86 (22.9)	60 (24.0)	26 (20.8)	77 (34.8)
III	85 (22.7)	50 (20.0)	35 (28.0)	49 (22.2)
IV	5 (1.3)	4 (1.6)	1 (0.8)	0 (0)
NA	24 (6.4)	16 (6.4)	8 (6.4)	2 (0.91)

*, cases were staged according to the American Joint Committee on Cancer (AJCC) (8th) (26). HCC, hepatocellular carcinoma; LIHC, liver hepatocellular carcinoma; NA, not available.

located were also shown in the Table S2. Both cg05373863 and cg13028471 were annotated to the same gene SLC7A11. Therefore, we applied the corresponding genes to construct the ferroptosis-related transcriptional score using similar method: $Score_{gene\ expression}$ =0.42× PGD +0.40× SLC7A11+0.17× ZEB1–0.16× ACACA. The associations between CpG sites and corresponding gene expressions were listed in Table S3.

Combination and evaluation of ferroptosis-related epigenetic and transcriptional score

We then performed Kaplan-Meier survival analysis to determine the difference according to the signature in total set, including methylation score, transcriptional score, integrative score (methylation score + transcriptional score) and prognostic score (clinical information + methylation score + transcriptional score). Subjects were dichotomized as high-risk group and low-risk group using the median score. In the total set, we found that the high-risk group had significant shorter survival time than the low-risk group in four signatures (methylation score: HR =3.29, 95% CI: 2.06–5.24, P=5.47E-07; transcriptional score: HR =1.65, 95% CI: 1.08–2.52, P=2.04E-02; integrative score: HR =2.64, 95% CI: 1.69–4.13, P=2.09E-05; prognostic score: HR =2.72, 95% CI: 2.01–3.68, P=8.75E-11, *Figure 2*).

To further validate our findings, an independent dataset was used in the validation. The transcription score demonstrated that high-risk group had significant shorter survival time than low-risk group (HR =2.72, 95% CI: 1.19–6.20, P=0.0175, log-rank P=0.0098, Figure S1). However, the methylation data in this dataset is not available.

The area under curve (AUC) of 3- and 5-year survival for HCC

The prognostic signature integrating epigenetic (DNA methylation), transcriptional (gene expression), and clinical omics level (clinical information), was found to have the best predictive capability than other scores. Compared with the model using clinical data with gene expression (AUC1 of 3-year survival =0.602), the model combining clinical information, expression, and methylation data (AUC3 of 3-year survival =0.617) performed best for 3-year survival prediction [AUC3 *vs.* AUC1: 7.00% (95% CI: 6.62%, 7.40%), P<2.20E-16, *Figure 3A*]. The superior prediction ability of multi-omics model (AUC3 of 5-year survival =0.636) was more apparent in 5-year survival prediction, compared with others [AUC3 *vs.* AUC1: 14.26% (95% CI: 13.82%, 14.70%), P<2.20E-16, *Figure 3B*].

Mediation analysis of ferroptosis-related methylation and transcriptional score

According to published literature (27), we proposed that the prognostic value of DNA methylation was mediated by affecting their corresponding gene expression. Therefore, we combine the four genes' mRNA expression

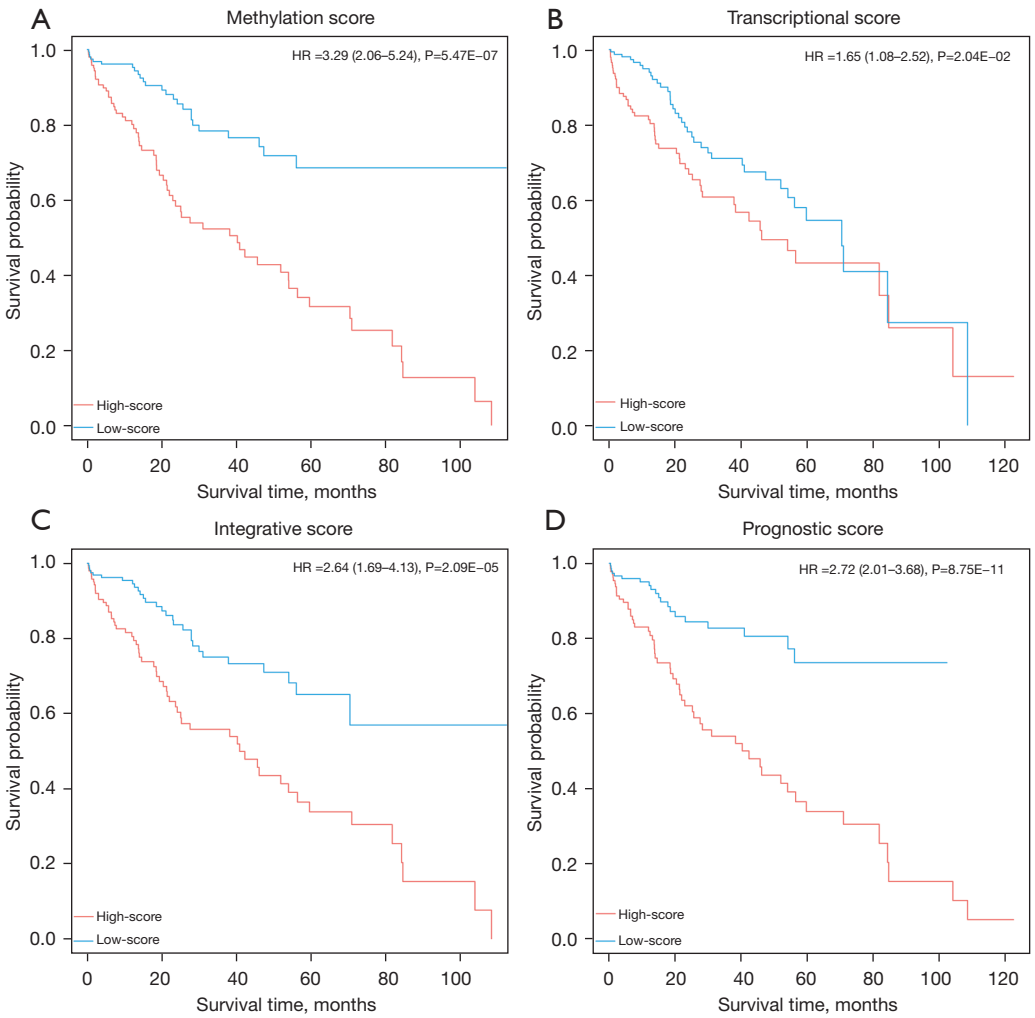

Figure 2 Kaplan-Meier survival curves of various prognostic signature scores. (A) Methylation score of DNA methylation (HR =3.29, 95% CI: 2.06–5.24, P=5.47E-07). (B) Transcriptional score of gene expression (HR =1.65, 95% CI: 1.08–2.52, P=2.04E-02). (C) Integrative score combining DNA methylation and gene expression (HR =2.64, 95% CI: 1.69–4.13, P=2.09E-05). (D) Prognostic score integrating DNA methylation, gene expression, and clinical information (HR =2.72, 95% CI: 2.01–3.68, P=8.75E-11). Patients were dichotomized into low-risk, and high-risk groups using the median as the cutoff value. HR, hazard ratio.

as ferroptosis-related transcriptional score (as mentioned above: $Score_{gene\ expression}$), which was regarded as mediated variant between DNA methylation and overall survival. Interestingly, our results validated the hypothesis ($HR_{indirect}$ =1.07, 95% CI: 1.02–1.14, P=7.65E-03; proportion mediated: 24.77%, *Figure 4*), which remained statistically significant after sensitivity analysis by excluding each gene expression from $Score_{gene\ expression}$.

Discussion

In the current study, we conducted a multi-stage screening strategy to identify significant ferroptosis-related DNA methylation CpG sites associated with survival employing multi-omics data and clinical data from TCGA. The ferroptosis-related methylation score of 5 candidate CpG sites and transcriptional score of corresponding gene expression independently presented superior prediction performance of HCC patients' prognosis. We then constructed a novel prognostic model integrating five DNA methylation CpG sites, four genes corresponding to CpG sites and clinical variables. Mediation analysis further indicated the possible mechanism implicating how DNA methylation affecting overall survival of HCC patients.

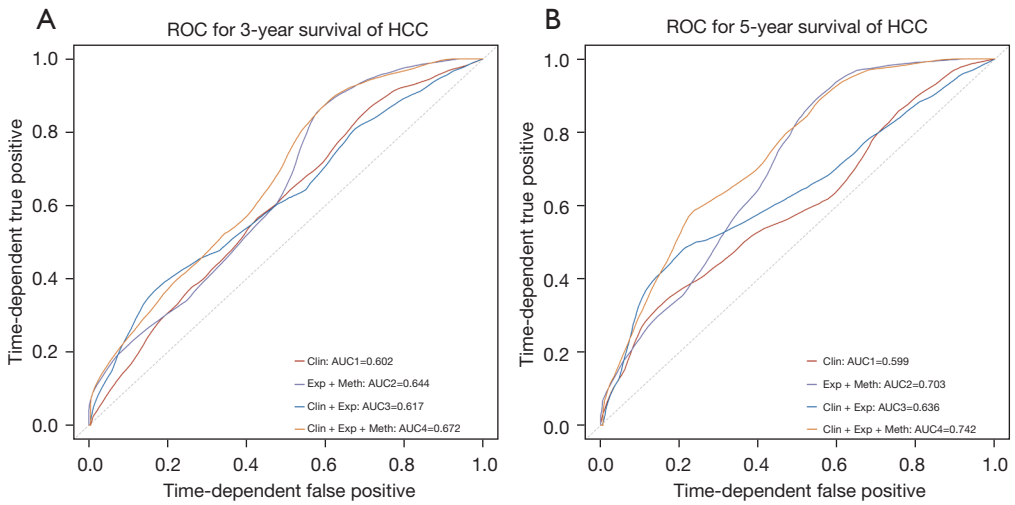

Figure 3 ROC for multiple predictive signatures using the clinical information, the main and interaction effects of DNA methylation, and gene expression. (A) ROCs of multiple predictive signatures for 3-year survival. (B) ROCs of multiple predictive signatures for 5-year survival. ROC, receiver operating characteristic curves; HCC, hepatocellular carcinoma; AUC, area under the receiver operating characteristic curve.

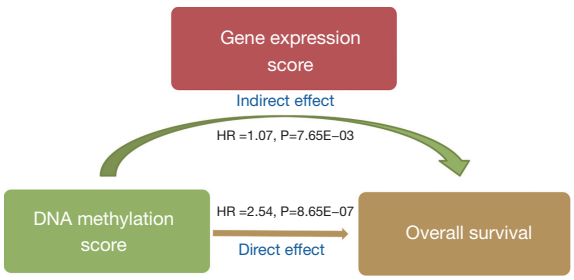

Figure 4 Diagram of mediation model—mediation analysis for methylation-based signature through mRNA expression. HR, hazard ratio.

Although previous studies (17,28) have reported the potential role of FRGs in predicting prognosis of several types of cancer, including HCC. The prognostic value of DNA methylation on CpG sites, which might contribute to aberrant expression of target genes, remains largely unknown. In this study, the ferroptosis-related methylation score constructed from 5 candidate CpG sites performed well in the prediction of overall survival in HCC patients. High-risk group has 2.29 times higher death risk than the low-risk group. The transcriptional score including four corresponding gene expression has similar performance in overall survival prediction in validation dataset. These results indicated the prognostic role of FRGs in HCC and the potentiality to build a multi-omics prognostic model. Ferroptosis is a unique modality of cell death driven by metabolic dysfunctions involving ROS, iron, and polyunsaturated fatty acids (PUFAs), multiple genes and signaling pathways participate in ferroptosis, such as lipid synthesis, metabolism in iron or energy, and oxidative stress. Notably, SLC7A11 is the corresponding gene of two identified CpG sites in our study, which was coincidentally included in several prognosis model of HCC patients proposed by previous studies (17,29). SLC7A11, considered as a subunit of system X_c^-, which could import cystine into the cell, sensitize fibrosarcoma cells to ferroptosis (30). The study by Jiang and colleagues found that p53 can potentiate ferroptosis via suppressing the transcription of SLC7A11, and this function may contribute to the tumor-suppressive function of p53, which indicated the potential mechanism between ferroptosis and HCC prognosis (31). Similar to p53, the tumor-suppressor activity of BAP1 is also partly mediated by ferroptosis through repression of SLC7A11 (32). ACACA encodes ACC1, impacts the rate-limiting step in fatty acid synthesis during lipid metabolism, and it is also a substantial regulator of survival in tumor cell. Knockdown of ACACA could suppress CIL56-induced, but not erastin or RSL3 induced ferroptosis (33). According to our results, high methylation score is associated with high methylation of cg15044146 in ACACA, which results in resistance to ferroptosis and poor prognosis. This is inconsistent with previous studies (33,34). ZEB1 is an epithelial-mesenchymal transition (EMT) regulator as well as a lipogenic factor, could suppress GPX4 depletion-

induced ferroptosis (35). Phosphogluconate dehydrogenase (PGD), involved in the pentose phosphate pathway, has been reported to suppress erastin-induced ferroptosis in non-small cell lung cancer cell line Calu-1 (7). Our result suggested that methylation in cg02916418 site leads to low *PGD* gene expression, which associated with better survival of HCC. Therefore, the four genes in our prognostic signature were actively participated in the ferroptosis of cancer, targeting identified CpG sites in these genes could improve the outcomes of HCC patients.

Multiple models have been proposed in the prediction of prognosis in HCC patients (17,36). Single-cell omics data was applied reflecting genetic, epigenetic and transcriptomic heterogeneity in HCC (37). However, no model has incorporated epigenetic, transcriptomic and clinical factors in predicting outcomes in HCC patients. In our study, the integrated model performed apparently better than other models in both 3- and 5-year survival prediction. Based on the mediation analysis, we found that 24.77% prognostic effect of DNA methylation was mediated by affecting their corresponding gene expression in HCC patients, which partly explained the underlying mechanism of our model. The rest of 75.23% effect could be mediated by other factors, like promoter methylation induced gene function alterations (27).

There are several limitations of this study. First, this is a retrospective study using multi-omic data from public databases, no independent validation was applied. Only methylation score was validated using another independent dataset as we failed to find a dataset including both methylation and transcription data in HCC (20). Thus, the association should be interpreted with caution and prospective cohort data are warranted for further investigation to verify its clinical utility. Second, we only considered ferroptosis-related hallmark to build a prognostic model, and we did not consider other prominent prognostic genes in HCC. However, our model achieved moderate performance, indicating its robustness in predicting HCC outcomes, though further validation is still warranted. In addition, the relationship among DNA methylation, gene expression, and overall survival still lacks biological evidence, therefore, more research is warranted.

Conclusions

In conclusion, we established a novel trans-omics prognostic model involving 5 ferroptosis-related CpG sites and 4 corresponding genes which could predict overall survival of HCC. The identified CpG sites were potentially functional and targetable, indicating new avenues for individualized treatment of HCC patients.

Acknowledgments

We acknowledge all the participants involved in this study. *Funding*: This study was supported by Natural Science Foundation of Zhejiang Province (No. LY20H160026).

Footnote

Reporting Checklist: The authors have completed the TRIPOD reporting checklist. Available at https://tcr.amegroups.com/article/view/10.21037/tcr-21-2882/rc

Peer Review File: Available at https://tcr.amegroups.com/article/view/10.21037/tcr-21-2882/prf

Conflicts of Interest: All authors have completed the ICMJE uniform disclosure form (available at https://tcr.amegroups.com/article/view/10.21037/tcr-21-2882/coif). The authors have no conflicts of interest to declare.

Ethical Statement: The authors are accountable for all aspects of the work in ensuring that questions related to the accuracy or integrity of any part of the work are appropriately investigated and resolved. The study was conducted in accordance with the Declaration of Helsinki (as revised in 2013).

References

1. Sung H, Ferlay J, Siegel RL, et al. Global Cancer Statistics 2020: GLOBOCAN Estimates of Incidence and Mortality Worldwide for 36 Cancers in 185 Countries. CA Cancer J Clin 2021;71:209-49.
2. Islami F, Ward EM, Sung H, et al. Annual Report to the

Nation on the Status of Cancer, Part 1: National Cancer Statistics. J Natl Cancer Inst 2021;113:1648-69.
3. Njei B, Rotman Y, Ditah I, et al. Emerging trends in hepatocellular carcinoma incidence and mortality. Hepatology 2015;61:191-9.
4. Jemal A, Ward EM, Johnson CJ, et al. Annual Report to the Nation on the Status of Cancer, 1975-2014, Featuring Survival. J Natl Cancer Inst 2017;109:djx030.
5. Feng J, Zhu R, Feng D, et al. Prediction of Early Recurrence of Solitary Hepatocellular Carcinoma after Orthotopic Liver Transplantation. Sci Rep 2019;9:15855.
6. Yang JD, Hainaut P, Gores GJ, et al. A global view of hepatocellular carcinoma: trends, risk, prevention and management. Nat Rev Gastroenterol Hepatol 2019;16:589-604.
7. Dixon SJ, Lemberg KM, Lamprecht MR, et al. Ferroptosis: an iron-dependent form of nonapoptotic cell death. Cell 2012;149:1060-72.
8. Nie J, Lin B, Zhou M, et al. Role of ferroptosis in hepatocellular carcinoma. J Cancer Res Clin Oncol 2018;144:2329-37.
9. Stockwell BR, Friedmann Angeli JP, Bayir H, et al. Ferroptosis: A Regulated Cell Death Nexus Linking Metabolism, Redox Biology, and Disease. Cell 2017;171:273-85.
10. Louandre C, Marcq I, Bouhlal H, et al. The retinoblastoma (Rb) protein regulates ferroptosis induced by sorafenib in human hepatocellular carcinoma cells. Cancer Lett 2015;356:971-7.
11. Jennis M, Kung CP, Basu S, et al. An African-specific polymorphism in the TP53 gene impairs p53 tumor suppressor function in a mouse model. Genes Dev 2016;30:918-30.
12. Manz DH, Blanchette NL, Paul BT, et al. Iron and cancer: recent insights. Ann N Y Acad Sci 2016;1368:149-61.
13. Xie Y, Hou W, Song X, et al. Ferroptosis: process and function. Cell Death Differ 2016;23:369-79.
14. Sun X, Ou Z, Chen R, et al. Activation of the p62-Keap1-NRF2 pathway protects against ferroptosis in hepatocellular carcinoma cells. Hepatology 2016;63:173-84.
15. Liu Z, Zhao Q, Zuo ZX, et al. Systematic Analysis of the Aberrances and Functional Implications of Ferroptosis in Cancer. iScience 2020;23:101302.
16. Shen S, Wang G, Shi Q, et al. Seven-CpG-based prognostic signature coupled with gene expression predicts survival of oral squamous cell carcinoma. Clin Epigenetics 2017;9:88.
17. Liang JY, Wang DS, Lin HC, et al. A Novel Ferroptosis-related Gene Signature for Overall Survival Prediction in Patients with Hepatocellular Carcinoma. Int J Biol Sci 2020;16:2430-41.
18. Liu Y, Zhang X, Zhang J, et al. Development and Validation of a Combined Ferroptosis and Immune Prognostic Classifier for Hepatocellular Carcinoma. Front Cell Dev Biol 2020;8:596679.
19. Cancer Genome Atlas Research Network. Electronic address: wheeler@bcm.edu; Cancer Genome Atlas Research Network. Comprehensive and Integrative Genomic Characterization of Hepatocellular Carcinoma. Cell 2017;169:1327-1341.e23.
20. Wang C, Liao Y, He W, et al. Elafin promotes tumour metastasis and attenuates the anti-metastatic effects of erlotinib via binding to EGFR in hepatocellular carcinoma. J Exp Clin Cancer Res 2021;40:113.
21. Pineda S, Real FX, Kogevinas M, et al. Integration Analysis of Three Omics Data Using Penalized Regression Methods: An Application to Bladder Cancer. PLoS Genet 2015;11:e1005689.
22. Fan J, Lv J. Sure independence screening for ultrahigh dimensional feature space (with discussion). J R Stat Soc, Ser B 2008;70:849–911.
23. Heagerty PJ, Zheng Y. Survival model predictive accuracy and ROC curves. Biometrics 2005;61:92-105.
24. Richiardi L, Bellocco R, Zugna D. Mediation analysis in epidemiology: methods, interpretation and bias. Int J Epidemiol 2013;42:1511-9.
25. Dong X, Zhang R, He J, et al. Trans-omics biomarker model improves prognostic prediction accuracy for early-stage lung adenocarcinoma. Aging (Albany NY) 2019;11:6312-35.
26. Chun YS, Pawlik TM, Vauthey JN. 8th Edition of the AJCC Cancer Staging Manual: Pancreas and Hepatobiliary Cancers. Ann Surg Oncol 2018;25:845-7.
27. Schübeler D. Function and information content of DNA methylation. Nature 2015;517:321-6.
28. Liu HJ, Hu HM, Li GZ, et al. Ferroptosis-Related Gene Signature Predicts Glioma Cell Death and Glioma Patient Progression. Front Cell Dev Biol 2020;8:538.
29. Tang B, Zhu J, Li J, et al. The ferroptosis and iron-metabolism signature robustly predicts clinical diagnosis, prognosis and immune microenvironment for hepatocellular carcinoma. Cell Commun Signal 2020;18:174.
30. Zhang Y, Shi J, Liu X, et al. BAP1 links metabolic regulation of ferroptosis to tumour suppression. Nat Cell Biol 2018;20:1181-92.
31. Jiang L, Kon N, Li T, et al. Ferroptosis as a p53-mediated

activity during tumour suppression. Nature 2015;520:57-62.
32. Hassannia B, Vandenabeele P, Vanden Berghe T. Targeting Ferroptosis to Iron Out Cancer. Cancer Cell 2019;35:830-49.
33. Dixon SJ, Winter GE, Musavi LS, et al. Human Haploid Cell Genetics Reveals Roles for Lipid Metabolism Genes in Nonapoptotic Cell Death. ACS Chem Biol 2015;10:1604-9.
34. Zhao GJ, Wu Z, Ge L, et al. Ferroptosis-Related Gene-Based Prognostic Model and Immune Infiltration in Clear Cell Renal Cell Carcinoma. Front Genet 2021;12:650416.
35. Viswanathan VS, Ryan MJ, Dhruv HD, et al. Dependency of a therapy-resistant state of cancer cells on a lipid peroxidase pathway. Nature 2017;547:453-7.
36. Long J, Chen P, Lin J, et al. DNA methylation-driven genes for constructing diagnostic, prognostic, and recurrence models for hepatocellular carcinoma. Theranostics 2019;9:7251-67.
37. Hou Y, Guo H, Cao C, et al. Single-cell triple omics sequencing reveals genetic, epigenetic, and transcriptomic heterogeneity in hepatocellular carcinomas. Cell Res 2016;26:304-19.

Cite this article as: Chen J, Zhu X, Chen D, Jin L, Xu W, Yu W, Zhang L. A multiomic ferroptosis-associated prognostic signature incorporating epigenetic and transcriptional biomarkers for hepatocellular carcinoma. Transl Cancer Res 2022;11(7):1889-1897. doi: 10.21037/tcr-21-2882

Supplementary

Table S1 60 Ferroptosis-related genes

Ferroptosis-related genes	Name
ACSL4	acyl-CoA synthetase long-chain family member 4
AKR1C1	aldo-keto reductase family 1 member C1
AKR1C2	aldo-keto reductase family 1 member C2
AKR1C3	aldo-keto reductase family 1 member C3
ALOX15	arachidonate 15-lipoxygenase
ALOX5	arachidonate 5-lipoxygenase
ALOX12	arachidonate 12-lipoxygenase
ATP5MC3	ATP synthase membrane subunit c locus 3
CARS	cysteinyl tRNA synthetase
CBS	cystathionine beta synthase
CD44	CD44 molecule
CHAC1	ChaC glutathione- specific gamma-glutamyl cyclotransferase 1
CISD1	CDGSH iron sulfur domain 1
CS	citrate synthase
DPP4	dipeptidyl-dippeptidase-4
FANCD2	Fanconi anemia complementation group D2
GCLC	glutamate-cysteine ligase catalytic subunit
GCLM	glutamate-cysteine ligase modifier subunit
GLS2	glutaminase 2
GPX4	glutathione peroxidase 4
GSS	glutathione synthetase
HMGCR	3-hydroxy-3-methylglutaryl-CoA reductase
HSPB1	heat shock protein beta 1
CRYAB	heat shock protein beta 5
LPCAT3	lysophosphatidylcholine acyltransferase 3
MT1G	metallothionein-1G
NCOA4	nuclear receptor coactivator 4
PTGS2	prostaglandin-endoperoxide synthase 2
RPL8	ribosomal protein L8
SAT1	spermidine/spermine N1-acetyltransferase 1
SLC7A11	solute carrier family 7 member 11
FDFT1	farnesyl-diphosphate farnesyltransferase 1
TFRC	transferrin receptor
TP53	tumor protein 53
EMC2	ER membrane protein complex subunit 2
AIFM2	apoptosis inducing factor mitochondria associated 2
PHKG2	phosphorylase kinase, g2
HSBP1	heat-shock 27-k Da protein 1
ACO1	aconitase 1
FTH1	ferritin heavy chain 1
STEAP3	six-transmembrane epithelial antigen of prostate 3
NFS1	cysteine desulfurase
ACSL3	acyl-CoA synthetase long-chain family member 3
ACACA	Acetyl-CoA carboxylase alpha
PEBP1	phosphatidylethanolamine-binding protein 1
ZEB1	zinc finger E-box-binding homeobox 1
SQLE	squalene monooxygenase
FADS2	fatty acid desaturase 2/acyl-CoA 6-desaturase
NFE2L2	nuclear factor, erythroid 2 like 2
KEAP1	kelch-like ECH- associated protein 1
NQO1	quinone oxidoreductase-1
NOX1	NADPH oxidase 1
ABCC1	ATP binding cassette subfamily C member 1
SLC1A5	solute carrier family 1 member 5
GOT1	glutamic-oxaloacetic transaminase 1
G6PD	glucose-6-phosphate dehydrogenase
PGD	phosphoglycerate dehydrogenase
IREB2	iron response element-binding protein 2
HMOX1	heme oxygenase 1
ACSF2	acyl-CoA synthetase family member 2

Table S1 (*continued*)

Table S1 (*continued*)

https://dx.doi.org/10.21037/tcr-21-2882

Table S2 Gene Symbol of 5 CpGs in the model

CpGs	Gene symbol
cg02916418	*PGD*
cg05373863	*SLC7A11*
cg07137701	*ZEB1*
cg13028471	*SLC7A11*
cg15044146	*ACACA*

Table S3 correlation analysis of gene expression and methylation

CpGs	Gene symbol	r	P
cg02916418	*PGD*	-0.45	1.39E-19
cg05373863	*SLC7A11*	-0.07	2.07E-01
cg07137701	*ZEB1*	0.10	4.60E-02
cg13028471	*SLC7A11*	-0.16	1.63E-03
cg15044146	*ACACA*	-0.02	7.25E-01

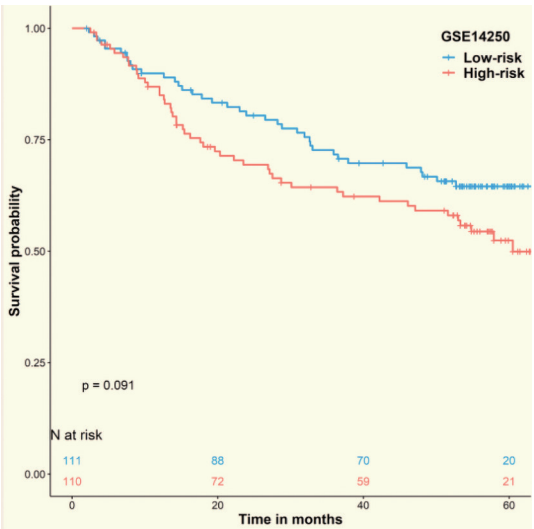

Figure S1 The transcription score was validated in an independent dataset GSE14250, which demonstrated that high-risk group had significant shorter survival time than low-risk group (HR =2.72, 95% CI: 1.19–6.20, P=0.0175, log-rank P=0.0098).

https://dx.doi.org/10.21037/tcr-21-2882